Experimental study of superharmonic internal wave resonant triads in finite-depth nonuniform stratifications

Dheeraj Varma [1,*] Corentin Pacary [1] Thierry Dauxois [1] and Sylvain Joubaud [1,2]

[1] *ENS de Lyon, CNRS, Laboratoire de Physique, F-69342 Lyon, France*
[2] *Institut Universitaire de France (IUF), 75231 Paris Cedex 05, France*

We present an experimental study on the excitation of superharmonic internal wave by resonant interaction of internal wave modes in finite-depth nonuniform stratifications. In a nonuniform stratification, the primary wave field composed of a single horizontally propagating vertical mode or combination of two horizontally propagating vertical modes is forced from one end of the tank using the wave generator at a forcing frequency ω_0. The spontaneous excitation of a superharmonic wave at frequency $2\omega_0$ by resonant interaction of the internal wave modes of the primary wave field forced at frequency ω_0 is observed. We experimentally demonstrate that even an isolated single mode could resonantly interact with itself to excite a superharmonic wave at frequency $2\omega_0$ in a nonuniform stratification, which is inhibited in the case of a uniform stratification. The resonant peak frequencies at which the strength of superharmonic signal is maximum, and the corresponding vertical structure of the superharmonic internal wave mode, qualitatively agree well with the theoretical predictions obtained from the weakly nonlinear analysis. The paper concludes with a discussion on experiments performed to observe superharmonic triadic resonant interactions in an oceanlike nonuniform stratification profile, for which the excited superharmonic internal wave modes were found to be trapped within the pycnocline region.

I. INTRODUCTION

Internal waves generated at spatially localized regions in the ocean due to barotropic tidal flow over bottom topography can be represented as horizontally propagating vertical modes at the tidal frequency, which ensures that the boundary conditions on the ocean floor and the free surface (often modeled as a rigid lid) are satisfied [1]. Vertical modes satisfy the no normal flow boundary condition at the ocean floor and the free surface of the ocean, with mode-*m* corresponding to a mode shape (vertical eigen function) having $m + 1$ zero crossings in the vertical direction. Low modes detected from satellite altimetry are observed to propagate larger distance (as far as 1000 km for mode-1) from generation sites [2,3], whereas high modes associated with higher shear dissipate locally near the generation sites [4]. As the low modes propagate, they transport both energy and momentum, and can transfer energy to higher modes due to scattering by further ocean bottom topography [5] and continental shelves [6]. Internal waves could also dissipate energy due to interactions with mean flows and due to buoyancy-driven and shear-driven instabilities [7]. Another potential mechanism through which energy from far-propagating low-mode internal tides could get transferred to shorter length and timescales are wave-wave interactions, such as the triadic resonant interactions [8–10].

Three interacting internal waves satisfying the relations $\mathbf{k_1} \pm \mathbf{k_2} \pm \mathbf{k_3} = \mathbf{0}$ and $\omega_1 \pm \omega_2 \pm \omega_3 = 0$ form a resonant triad, where $\mathbf{k_{1,2,3}}$ are the wave vectors and $\omega_{1,2,3}$ are the corresponding frequencies

---

*Contact author: nldvrm@gmail.com

obtained from the linear internal wave dispersion relation [11]. These aforementioned relations are referred to as the spatial and temporal resonant triad conditions. Most studies on triadic resonant interactions have focused on triadic resonant instability [11–15] in a uniform stratification, where one primary wave at frequency ω_0 gets unstable by exciting two secondary waves at subharmonic frequencies ($<\omega_0$), also referred to as subharmonic triadic resonance [15]. The first experimental evidence of subharmonic triadic resonance or triadic resonant instability in internal waves was shown by Davis and Acrivos [12]. Considering a stratified thin layer between two constant density layers in their experiments, Davis and Acrivos [12] observed that a mode-1 internal wave above a threshold amplitude, succumbs to a subharmonic instability with the secondary wave frequencies being noticeably different from half the primary wave frequency.

Another possible manifestation of triadic resonance is when two internal waves of the same frequency present in the primary wave field, excite a third wave as the secondary wave field due to triadic resonant interactions, referred to as superharmonic triadic resonance [15]. In a first theoretical study on internal wave modes in a finite-depth uniform stratification, Thorpe [16] computed the resonant frequency (i.e., the forcing frequency at which three interacting waves satisfy the resonant triad conditions) at which two horizontally propagating vertical internal waves mode-m and mode-n (where m and n are the mode numbers) in the primary wave field at frequency ω_0 are in triadic resonance with mode-$|m-n|$ at frequency $2\omega_0$. The theoretically identified resonant frequencies [16] at which superharmonic triadic resonance occurs have been validated in numerical simulations by Varma *et al.* [17] and in laboratory experiments by Husseini *et al.* [18]. Both aforementioned studies also captured the initial spatial evolution of the internal wave modes in the resonant triad to be in quantitatively good agreement with the theoretical predictions based on the amplitude evolution equations [17,18]. Excitation of superharmonics due to resonant interactions has also been observed in a more recent experimental study with an axisymmetric confined geometry for a uniform stratification [19].

Thorpe [20] considered a simpler two layer model, a mixed layer above a uniformly stratified fluid layer, to show that higher harmonic internal waves can be excited when an upward propagating internal wave (in uniformly stratified fluid layer) impinges at the interface between the two layers. McHugh [21] generalized the aforementioned theoretical study by considering a two layer model with two uniformly stratified fluid layers of different buoyancy frequency, to show the generation of higher harmonics at the interface boundary due to nonlinear interactions of internal waves. While the generation of superharmonics in a continuous nonuniform stratification has received attention more recently in theoretical studies [22–26], experimental studies [27–29] and numerical simulations [17,30–34], to the best of our knowledge no previous experimental studies on internal waves have identified superharmonic resonant triads arising from nonlinear interactions of internal wave modes in a finite-depth nonuniform stratification. Experimental studies [27–29] and numerical simulations [30,31] on nonlinear interactions of internal waves in a nonuniform stratification, consider their primary wave field to be locally forced in some part of the vertical fluid column, i.e., internal wave beams, impinging on a pycnocline to excite higher harmonics in the pycnocline region due to nonlinear interactions.

In a nonuniform stratification, an isolated primary internal wave at frequency ω_0 could interact with itself (form hereon referred to as self-interaction) to excite a secondary wave at frequency $2\omega_0$, which is inhibited in a uniform stratification [16]. Considering an isolated internal wave mode in a nonuniform stratification, Sutherland [32] performed numerical simulations and demonstrated that self-interaction of internal wave modes can excite superharmonic internal waves through superharmonic triadic resonance. Under the weakly nonlinear theoretical framework, earlier theoretical studies [22–24] have identified the conditions under which self-interacting primary internal wave modes would excite superharmonic internal waves in oceanlike nonuniform stratifications. Varma and Mathur [23] considered a more general scenario in which two different modes in the primary wave field at a given frequency ω_0, would excite a third mode at the superharmonic frequency $2\omega_0$ due to superharmonic triadic resonance. Varma *et al.* [17] performed numerical simulations considering an oceanlike nonuniform stratification profile with a pycnocline, to show self-interaction
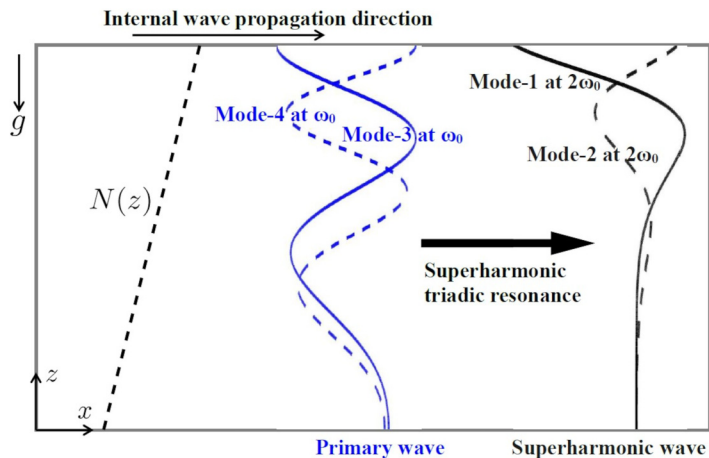
FIG. 1. Schematic representation of our experimental study of superharmonic triadic resonance in an idealized nonuniform stratification. The primary horizontal velocity wave field is either an isolated mode or a combinations of two different modes at ω_0 (mode-3 and/or mode-4), and their resonant interaction leads to excitation of a superharmonic internal wave mode at $2\omega_0$ (mode-1 or mode-2).

of mode-3 at and around the resonant frequency, resulting in excitation mode-1 superharmonics. Numerical simulations by Baker and Sutherland [33] showed nonlinear self-interaction of a mode-1 internal tide in a nonuniform stratification to excite mode-1 superharmonics at moderately different from twice the internal tide frequency. In more recent numerical simulations by Sutherland and Dhaliwal [34] with stronger nonlinear forcing, superharmonic cascade of energy from primary mode-1 to mode-1 higher harmonics was observed.

The focus of this paper, as shown in the schematic Fig. 1, is to experimentally investigate superharmonic triadic resonance in a nonuniform stratification, resulting from resonant interaction of two distinct modes at a forcing frequency, from hereon referred to as cross-modal interaction, and also by a self-interaction of an isolated mode, resulting in excitation of a superharmonic mode at twice the forcing frequency. The spontaneously excited superharmonic internal wave mode at frequency $2\omega_0$ can be evanescent in some sections of the vertical fluid column (as shown in Fig. 1) depending on the stratification profile. In our experimental study two specific cases of superharmonic internal wave resonant triads are considered.

A. Cross-modal interaction

The primary wave field is composed of two internal wave modes, mode-3 and mode-4 at forcing frequency ω_0. Depending on the forcing frequency ω_0, mode-3 and mode-4 could resonantly interact to excite a mode-1 or mode-2 internal wave at the superharmonic frequency $2\omega_0$.

B. Self-interaction

The primary wave field has an isolated internal wave mode, mode-3 (or mode-4) at forcing frequency ω_0. Depending on the forcing frequency ω_0, the isolated mode could resonantly self-interact to excite a mode-1 or mode-2 internal wave at superharmonic frequency $2\omega_0$.

In Sec. II, we present a weakly nonlinear theory valid for any nonuniform stratification to evaluate the resonant frequency at which two distinct modes (or an isolated single mode) would interact to excite a superharmonic mode at twice the forcing frequency. The weakly nonlinear theory was developed in an earlier theoretical study by Varma and Mathur [23]. In a uniform stratification, modes (m, n) at ω_0 can resonantly interact to give only mode-$(|m - n|)$ at $2\omega_0$ [16], so there is no possibility for self-interaction $(m = n)$. But for a nonuniform stratification: (1) the

superharmonic mode at $2\omega_0$ need not be mode-$(|m - n|)$, thus allowing for many more triadic interactions and (2) self-interaction is also allowed [23]. Both the aforementioned possibilities are explored in the present experimental study, and the experimental results are validated with the theoretical findings for two specific forms of stratification profiles: (1) linear $N(z)$ profiles and (2) idealized ocean like Gaussian stratification profiles. The experimental apparatus and methods used are described in Sec. III. Mode-3 and mode-4 were the optimal choice for our experimental study as: (i) mode-1 and mode-2 have larger group velocities, and would travel faster and reflect back to the visualization window, allowing a smaller time window for analyzing the flow dynamics; (ii) considering higher modes (higher than mode-4) would introduce nonnegligible viscous effects. In Sec. IV, the experimental results are discussed for the two cases (i) cross-modal interaction and (ii) self-interaction. An oceanlike nonuniform stratification with a pycnocline is also considered making our study relevant for ocean, and both the aforementioned cases are investigated in Sec. V. The concluding remarks are presented in Sec. VI.

II. THEORY

For any arbitrary nonuniform stratification, the equations governing an inviscid, incompressible, nonrotating, two-dimensional flow within the Boussinesq approximation (LeBlond and Mysak [35]) are

$$\frac{\partial^2}{\partial t^2}\nabla^2\psi + N^2(z)\frac{\partial^2\psi}{\partial x^2} = \frac{\partial}{\partial x}[J(\psi, b)] - \frac{\partial}{\partial t}[J(\psi, \nabla^2\psi)], \tag{1}$$

$$\frac{\partial b}{\partial t} = -J(\psi, b) + N^2(z)\frac{\partial \psi}{\partial x}, \tag{2}$$

where $\psi(x, z, t)$ and $b(x, z, t)$ are the stream function and buoyancy perturbation, respectively. The background stratification is specified by the buoyancy frequency defined as $N(z) = \sqrt{(-g/\rho_{\rm ref})d\rho_0/dz}$, where gravity g acts along negative z, $\rho_{\rm ref}$ is a reference density and $\rho_0(z)$ is the background density profile. For laboratory experiments the reference density ($\rho_{\rm ref}$) is assumed to be the density of water $\rho_{\rm ref} = 1000\,{\rm kg/m^3}$. The Jacobian and Laplacian operators are defined as $J(A, B) = (\partial A/\partial x)(\partial B/\partial z) - (\partial B/\partial x)(\partial A/\partial z)$ and $\nabla^2 A = \partial^2 A/\partial x^2 + \partial^2 A/\partial z^2$, respectively. The velocity field is given by $(u, w) = (-\partial\psi/\partial z, \partial\psi/\partial x)$.

We consider a flow field given by a regular perturbation series in a small nonlinearity parameter ϵ (LeBlond and Mysak [35])

$$\psi(x, z, t) = \epsilon\psi_1(x, z, t) + \epsilon^2\psi_2(x, z, t) + \mathcal{O}(\epsilon^3), \tag{3}$$

$$b(x, z, t) = \epsilon b_1(x, z, t) + \epsilon^2 b_2(x, z, t) + \mathcal{O}(\epsilon^3), \tag{4}$$

representing perturbations to the background flow state described by a quiescent fluid with a stable stratification $N(z)$. The $\mathcal{O}(\epsilon)$ solution can be written as a linear superposition of right-propagating linear internal vertical modes [23] as

$$\psi_1 = \sum_{j=1}^{\infty}\frac{\Psi_j}{2}\phi_j(z)e^{i(k_j x - \omega_0 t)} + {\rm c.c.}, \tag{5}$$

where c.c. denotes complex conjugate. The complex modal amplitudes Ψ_j are assumed to be constant. The mode shapes $\phi_j(z)$, of horizontal wave number $k_j > 0$ and frequency ω_0 satisfy

$$\frac{d^2\phi_j}{dz^2} + \frac{k_j^2(N(z)^2 - \omega_0^2)}{\omega_0^2}\phi_j = 0, \tag{6}$$

with the mode shapes $\phi_j(z)$ satisfying the boundary conditions $\phi_j(z = 0) = \phi_j(z = H) = 0$, where H is the depth of the stratified fluid column.

$\mathcal{O}(\epsilon^2)$ solution results from the interaction of the terms of the linear solution [Jacobian terms in governing Eqs. (1) and (2)] and can be written as

$$\psi_2 = \sum_{m=1}^{\infty} \sum_{n=1}^{\infty} h_{mn}(z) e^{i[(k_m+k_n)x - 2\omega_0 t]} + g_{mn}(z) e^{i[(k_m-k_n)x]} + \text{c.c.}, \tag{7}$$

composed of terms with superharmonic waves at frequency $2\omega_0$ with horizontal wave number $k_m + k_n$, and time-independent standing waves with horizontal wave number $k_m - k_n$. The governing equation for $h_{mn}(z)$ of the the superharmonic wave at frequency $2\omega_0$ is

$$\frac{d^2 h_{mn}}{dz^2} + (k_m + k_n)^2 \frac{N^2(z) - 4\omega_0^2}{4\omega_0^2} h_{mn} = C_{mn}(z), \tag{8}$$

with $h_{mn}(z)$ satisfying the boundary conditions $h_{mn}(z=0) = h_{mn}(z=H) = 0$. The forcing term $C_{mn}(z)$ is a complicated analytical function which depends on the mode shapes $\phi_j(z)$, wave numbers k_j, stratification profile $N(z)$ and the forcing frequency ω_0. More details of the form of analytical functions, simplifications of the analytical functions, and the detailed derivations, valid for any arbitrary stratification $N(z)$, can be found in Varma and Mathur [23], and here, we refrain from showing the expressions of analytical functions.

For a given nonuniform stratification $N(z)$ and a given modal combination (m, n) at ω_0, $h_{mn}(z)$ is calculated numerically by solving Eq. (8) along with the boundary conditions as a boundary value problem using the in-built Matlab function bvp4c. The amplitude $h_{mn}^{\max} = \max[h_{mn}(z)]$ is computed for a range of forcing frequencies, to obtain the local maxima of $h_{mn}^{\max}$ and the associated frequency ω_{res}. The identified frequency ω_{res} is the resonant frequency at which mode-p (mode number associated with $h_{mn}(z)$) at superharmonic frequency $2\omega_0$, would be in triadic resonance with modes (m, n) at the forcing frequency ω_0, for a prescribed nonuniform stratification profile $N(z)$ [23]. This procedure is used to identify the resonant forcing frequencies for all the stratification profiles and the modal combinations considered in our experimental study. For a uniform stratification, i.e., $N(z)$ is constant, the mode number p of the superharmonic wave at $2\omega_0$ satisfies the condition $p = |m - n|$ [16]. Such a condition is not necessarily true for a nonuniform stratification as shown in a theoretical study by Varma and Mathur [23].

In Sec. IV, we consider a linear (nonuniform) stratification $N(z)$ profile specified by

$$\frac{N(z)}{N_{\min}} = 1 + (\beta - 1)\frac{z}{H}, \tag{9}$$

where $\beta = N_{\max}/N_{\min}$ is a characteristic measure of the slope of the stratification profile $N(z)$, used here as a proxy to measure its nonuniformity. Figure 2(a) shows the stratification profile considered as in Eq. (9) in a finite-depth water column of depth H. The nonuniform stratification profile considered is a linear $N(z)$ profile with the slope specified by $(\beta - 1)$. Depending on the forcing frequency $\omega_0 < N_{\min}$ or $\omega_0 > N_{\min}$, the internal wave modes can be propagating throughout the vertical fluid column or just in the upper section of the vertical fluid column, respectively. For $\beta = 3$, mode-3 and mode-4 at forcing frequency $\omega_0 = 0.9 N_{\min}$ are shown in Fig. 2(b), and as $\omega_0 < N_{\min}$ the modes are propagating in the entire depth. If $\omega_0 > N_{\min}$, then we observe a mode propagating only in the upper section of the vertical fluid column and is evanescent in the lower section of vertical fluid column as shown in Fig. 2(c), where mode-1 and mode-2 are forced at a forcing frequency $\omega_0 = 1.8 N_{\min}$.

We also consider an idealized oceanlike nonuniform stratification profile $N_1(z)$ with a pycnocline defined by

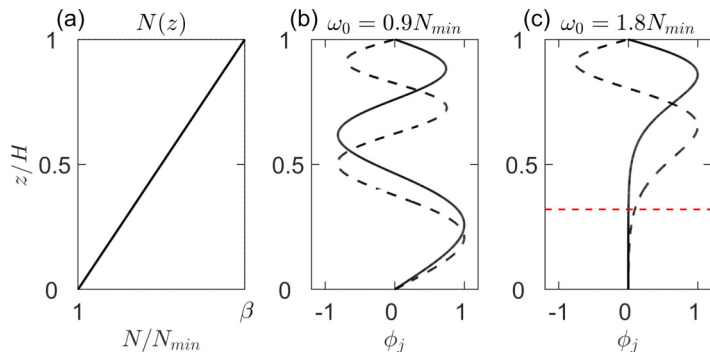$$\frac{N_1(z)}{N_{\min}} = 1 + (\beta - 1) \exp\left(-\frac{(z - z_c)^2}{\sigma^2}\right), \tag{10}$$

FIG. 2. (a) Linear (nonuniform) stratification profile as defined in Eq. (9), (b) mode-3 (solid curve) and mode-4 (dashed curve) propagating in the entire depth for forcing frequency $\omega_0 = 0.9N_{\min}$, and (c) mode-1 (solid curve) and mode-2 (dashed curve) propagate only in the upper section of the vertical fluid column above the red dashed line, and are evanescent in the lower section of the vertical fluid column for forcing frequency $\omega_0 = 1.8N_{\min}$ (the red dashed line corresponds to the z/H of cutoff frequency below which waves are evanescent). For panels (b) and (c), stratification profile as shown in Eq. (9) for $\beta = 3$ is considered.

where $N_{\min}$ is the deep ocean uniform stratification and z_c is the center of the pycnocline whose characteristic width is σ. More details of idealized oceanlike nonuniform stratification profile and the experimental observations are discussed in Sec. V.

III. EXPERIMENTAL APPARATUS AND METHODS

Experiments were performed in a thin long acrylic tank of 4 m length, 0.17 m width, and 0.4 m height, composed by joining 5 components of 0.8 m length, as shown in Fig. 3. The
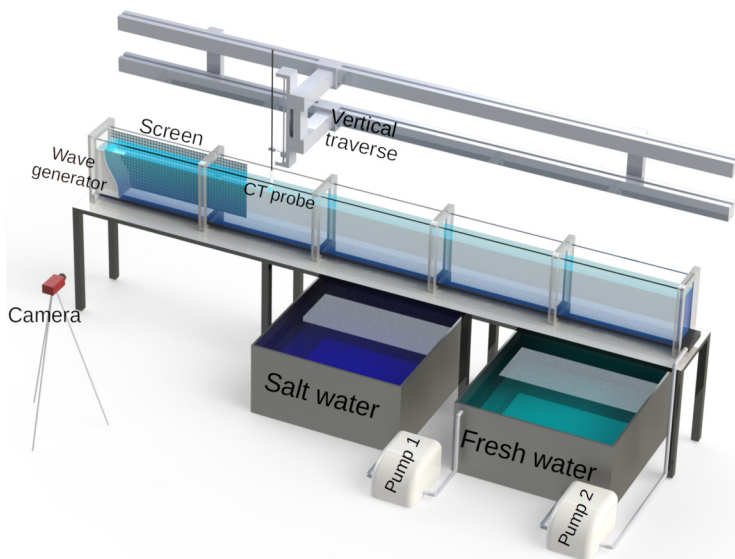

FIG. 3. Experimental setup with a 4 m long tank, filled with continuously varying density fluid using the double bucket method, with the two programmable pumps. The vertical density profile is measured by the vertically traversing CT probe, and internal wave modes of prescribed shape are forced by a wave generator on the left end, and the evolving flow field is captured by synthetic Schlieren technique.
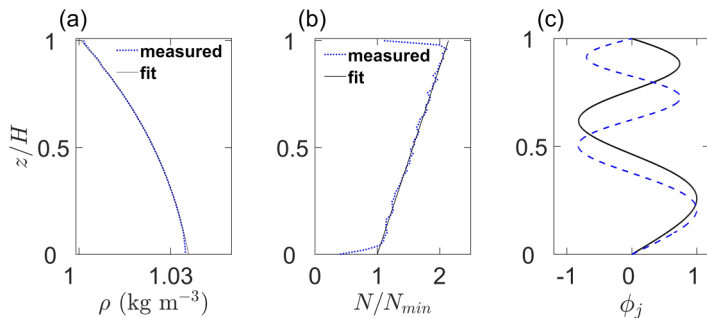
FIG. 4. (a) A measured density profile (blue dotted line) along with the fitted density profile (black solid line) corresponding to linear $N(z)$ fit, (b) a measured stratification profile (blue dotted line) along with the fitted $N(z)$ profile (black solid line) corresponding to $N(z)$ fit with $\beta = 2.1$ [as in Eq. (9)], and (c) mode-3 (black solid curve) and mode-4 (blue dashed curve) for $\beta = 2.1$ at $\omega_0/N_{\min} = 0.9$.

double-bucket method [36–38] is used to setup the prescribed nonuniform salt stratification over a depth of $H = 0.325\,\text{m}$ in the tank, by varying the flow rates of the computer programmable pump (pump 1 shown in Fig. 3) connecting the two buckets, while the pump 2 was maintained at constant flow rate. After filling the tank, the vertical density profile is measured by a vertically traversing conductivity-temperature (CT) probe (see Fig. 3), which is *a priori* calibrated using known density samples. A linear $N(z)$ profile defined by Eq. (9) was fit to the measured density profile by using the method of least squares to obtain β and $N_{\min}$. The experimental error in measurement of β is estimated to be around $3\%-5\%$, while computing the linear fit $N(z)$ profile. This error is associated to the presence of small mixed layers ($\approx 3\,\text{mm}$) at the free surface and bottom of the tank. For the set of experiments performed in this study, the stratification profiles were reproducible with certain differences in the upper few millimeters, which is associated to the mixed layer formation. Replicating the same stratification profile is achievable by carefully repeating the exact procedure and setting the same input parameters like pumps flow rates, initial volumes and initial densities of the two buckets. For all the experiments performed, $N(z = 0) = N_{\min}$ was fixed at $N_{\min} \approx 0.5\,\text{rad s}^{-1}$, and β was varied to investigate the shift in the resonant peak frequency, and change in mode number of the superharmonic wave both in the case of a mode propagating in the entire depth of the vertical fluid column and in the case of a mode propagating only in the upper section of the vertical fluid column. A representative measured density profile along with the fitted density profile corresponding to a linear $N(z)$ is shown in Fig. 4(a), and the corresponding fitted linear $N(z)$ profile for $\beta = 2.1$ is shown in Fig. 4(b). The mode shapes of the primary wave modes corresponding to the fitted linear $N(z)$ profile at forcing frequency $\omega_0/N_{\min} = 0.9$ are shown in Fig. 4(c).

The internal wave generator comprises 50 plates of 6.5 mm thickness each, each of which is independently driven by a motor. More details of the configuration of the wave generator can be found in previous experimental studies by Mercier *et al.* [39] and Dossmann *et al.* [40]. Each plate of the wave generator executes a constant amplitude horizontal oscillation, and the vertical profile of the horizontal displacement field at the wave generator location ($x = 0$) can be given by (t denotes time)

$$\Gamma_x(x = 0, z, t) = \left[A_m \frac{d\phi_m}{dz} + A_n \frac{d\phi_n}{dz} \right] \cos \omega_0 t, \qquad (11)$$

thus comprising left-to-right propagating modes m and n with amplitudes A_m and A_n, respectively at forcing frequency ω_0. Equation (6) is solved numerically as a boundary value problem (implementing $\phi(z = 0) = \phi(z = H) = 0$) with the measured fit $N(z)$ profile, and the prescribed internal wave forcing frequency ω_0, to obtain the mode shapes $\phi(z)$. The numerically obtained internal

TABLE I. Parameter values for all the experiments performed for linear nonuniform stratification specified by Eq. (9), and an oceanlike nonuniform stratification profile with a pycnocline specified by Eq. (12). Either a combination of modes (3, 4) or an isolated mode-3/mode-4 are the primary waves forced at the left end of the tank.

Stratification	Primary modes	β	$\omega_{\mathrm{res}}/N_{\mathrm{min}}$	mode at $2\omega_0$
Linear $N(z)$ profile	(3,4)	1.3	0.5703	1
$\frac{N(z)}{N_{\mathrm{min}}} = 1 + (\beta - 1)\frac{z}{H}$	(3,4)	1.6	0.6729	1
	(3,4)	1.8	0.7451	1
	(3,4)	2.1	0.8571	1
	(3,4)	2.2	0.8953	1
Linear $N(z)$ profile	(3,4)	2.1	0.6743	2
Linear $N(z)$ profile	3	2.1	0.8326	1
$\frac{N(z)}{N_{\mathrm{min}}} = 1 + (\beta - 1)\frac{z}{H}$	4	3	1.2368	1
Oceanlike $N_1(z)$ profile ($z_c/H = 0.8$ and $\sigma/H = 0.15$)	(3,4)	3	1.3705	1
$\frac{N_1(z)}{N_{\mathrm{min}}} = 1 + (\beta - 1)\exp\left(-\frac{(z-z_c)^2}{\sigma^2}\right)$	3	3	0.6842	2

wave modes at a fixed frequency ω_0 (time period $T_0 = 2\pi/\omega_0$), are then forced at the left end of the tank using the internal wave generator. For all the experiments performed A_m and A_n were fixed to be 5 mm, corresponding to fixed horizontal displacement amplitudes for all the forcing frequencies. For the case of self-interaction $m = n$, the forcing amplitude of an isolated mode would be 10 mm. In our experimental setup the wave generator plates cannot be displaced more than 10 mm and these amplitudes are also well-suited for examining weakly nonlinear interactions. Table I shows the details of all the experiments performed with varying β at resonant and off-resonant frequencies. The resonant frequencies $\omega_{\mathrm{res}}/N_{\mathrm{min}}$ were determined by analyzing the divergence in the superharmonic amplitude h_{mn} across a continuous range of frequencies for a specific modal combination (m, n), and a particular stratification profile prescribed by specifying β.

Synthetic Schlieren technique [41] is used to measure the density gradient fields. A CCD AVT Pike F-505 camera of resolution 2452×2054 pixels placed at a distance of $D = 2.8$ m from the front wall of the tank (as shown in Fig. 3), captures images (6 Hz) of the back-lit random pattern of dots of length $L = 1$ m placed behind the back wall of the tank at a distance of $d = 0.125$ m. For each of the captured images, the apparent displacement of the dots caused by the density gradient perturbations in the flow, with reference to the image captured without any flow, was estimated using correlation image velocimetry [42], implemented in the open source software UVMAT [43]. A quantitative measurement of the horizontal and vertical density gradient perturbation fields over a domain of 1 m in the horizontal and 0.325 m in the vertical was obtained as the final output of the image processing.

IV. RESULTS: LINEAR $N(z)$ PROFILE

In this section, we present the experimental and theoretical results, for the two cases considered: (i) cross-modal interaction of mode-3 and mode-4 at ω_0, and (ii) self-interaction of isolated mode-3 or isolated mode-4 at ω_0, in a nonuniform stratification specified by linear $N(z)$ profile shown in Eq. (9). We recall that the divergence of amplitude of superharmonic term in Eq. (7), i.e., $h_{mn}(z)$, for a given primary wave field composed of modes (m, n) at a frequency ω_0 allows us to identify the resonant peak frequency ω_{res} at which the resonant triad conditions get satisfied [23]. The resonant peak frequencies can thus be theoretically estimated in both of the aforementioned cases for any given value of β and modal combination (m, n).
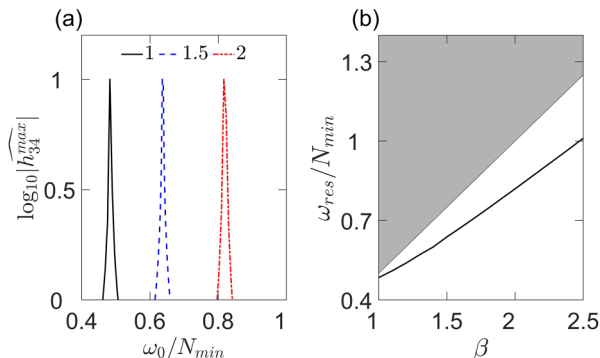
FIG. 5. (a) Variation of amplitude of the superharmonic mode-1 ($\log_{10} |h_{34}^{\max}|$) with $\omega_0/N_{\min}$ is plotted for three various values of $\beta = 1$ (black solid curve), 1.5 (blue dashed curve), and 2 (red dash-dotted curve), to identify the resonant peak frequency $\omega_{\mathrm{res}}/N_{\min}$ for each value of β. (b) Continuous variation of resonant peak frequency (solid curve) with β, corresponding to excitation of mode-1 superharmonic. Forcing frequencies for which superharmonic mode would be evanescent ($2\omega_0/N_{\min} > \beta$) is shown in gray color.

A. Cross-modal interaction

Cross-modal interaction of two internal wave modes (m, n) at frequency ω_0 in a uniform stratification can only result in excitation of mode-($p = |m - n|$) at the superharmonic frequency $2\omega_0$ [16]. But for a nonuniform stratification this specific criterion of mode-p excited at superharmonic frequency $2\omega_0$ satisfying $p = |m - n|$ is not necessary, as shown in the theoretical study of Varma and Mathur [23]. In the following Secs. IV A 1 and IV A 2, we show experimental observations of cross-modal interactions of mode-3 and mode-4 at frequency ω_0 resonantly exciting superharmonic mode-1 at frequency $2\omega_0$, and superharmonic mode-2 at frequency $2\omega_0$, respectively.

1. Superharmonic mode-1

For the case of cross-modal interaction, composed of primary internal wave modes, mode-3 and mode-4 at forcing frequency ω_0, the amplitude of the superharmonic mode-1 $|h_{34}(z)|$ [Eq. (8)] is numerically computed for a continuous range of forcing frequencies to identify the resonant peak frequency ω_{res} for a given β, as discussed in Sec. II. Figure 5(a) shows the variation of $\log_{10}|h_{34}^{\max}|$ with the forcing frequency for values of $\beta = 1$, $\beta = 1.5$, and $\beta = 2$, and a clear peak resonant frequency for mode-1 superharmonic could be observed for each value of β considered. As shown in Fig. 5(a), the resonant peak frequency shifts toward the right as the value of β increases. In Fig. 5(b), we plot the variation of resonant peak frequency of mode-1 superharmonic for a continuous range of values of β varying from 1 to 2.5. In the limit of $\beta = 1$, which corresponds to a uniform stratification, i.e., constant $N(z) = N_{\min}$, we recover the resonant frequency to be $\omega_{\mathrm{res}}/N_{\min} = 0.4841$ [18]. As shown in Fig. 5(b) by the solid line, the resonant peak frequency $\omega_{\mathrm{res}}/N_{\min}$ increases monotonically with increase in value of β, and the resonant peak frequency $\omega_{\mathrm{res}}/N_{\min}$ is always below the cutoff frequency regime [shown by gray region in Fig. 5(b)] in which the superharmonic wave would be completely evanescent ($2\omega_0/N_{\min} > \beta$).

In the experiments, a mode form corresponding to a combination of mode-3 and mode-4 ($A_3 = A_4 = 5\,\mathrm{mm}$), was forced for various values of forcing frequency ω_0, at the left end of the tank using the wave generator. The mode shapes were numerically obtained by solving Eq. (6) considering the corresponding nonuniform stratification profile measured using the CT probe. For a prescribed β, the range of forcing frequencies $\omega_0/N_{\min}$ were chosen at and around the theoretically identified resonant peak frequency $\omega_{\mathrm{res}}/N_{\min}$ (see Table I) corresponding to superharmonic mode-1, at which $h_{34}^{\max}$ diverges. The reason attributed to this choice of modal combination $(m, n) = (3, 4)$ is in respect to the experimental limitations of the tank length, the group velocities of the modes and a sufficient
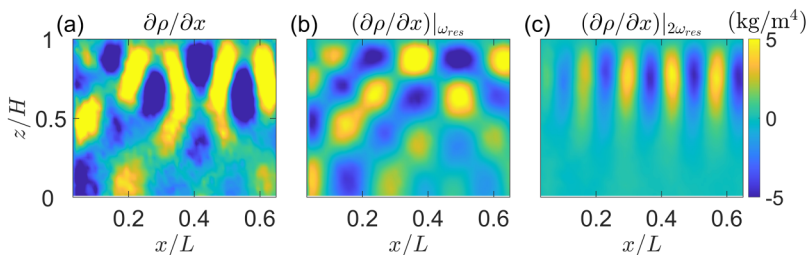
FIG. 6. Horizontal density gradient wave-fields for the cross-modal interaction, i.e., $(m, n, p) = (3, 4, 1)$, at the resonant forcing frequency of $\omega_{\text{res}}/N_{\min} = 0.8571$ for $\beta = 2.1$. (a) Instantaneous horizontal density gradient field, (b) Horizontal density gradient field filtered at the forcing frequency $\omega_{\text{res}}/N_{\min}$, and (c) Horizontal density gradient field filtered at the superharmonic frequency $2\omega_{\text{res}}/N_{\min}$. All the plots correspond to $t = 20T_0$, where $T_0 = 2\pi/\omega_{\text{res}}$.

time window for analysis. Mode-1 and mode-2 have higher group velocities compared to higher modes ($m > 2$), hence allowing a smaller time window before they get reflected back from the right end of the tank to reach the region of flow visualization. The time window $20T_0-25T_0$ was observed to be a reliable estimate for the analysis, which was long enough for the primary wave field to attain a constant amplitude, and not so long before the reflected wave reaches the flow visualization region. All the set of experiments performed with various values of β and forcing frequencies are shown in Table I. We now discuss one such set of experiments for a stratification profile with $\beta = 2.1$, which was shown in Fig. 4. For $\beta = 2.1$, the amplitude of superharmonic term in Eq. (7), i.e., $h_{34}(z)$ diverges at $\omega_{\text{res}}/N_{\min} = 0.8571$ corresponding to superharmonic mode-1 being excited at frequency $2\omega_{\text{res}}/N_{\min}$.

For the stratification profile setup with $\beta = 2.1$, mode-3 and mode-4 at $\omega_{\text{res}}/N_{\min} = 0.8571$ are forced at the left end of the tank using the wave generator. Figure 6(a) shows a snapshot of the instantaneous horizontal density gradient wave field at $t = 20T_0$, where $T_0 = 2\pi/\omega_{\text{res}}$. The horizontal density gradient field filtered at the forcing frequency $\omega_{\text{res}}/N_{\min} = 0.8571$ as shown in Fig. 6(b), displays a clean spatial structure of wave field corresponding to a superposition of mode-3 and mode-4 as forced from at $x = 0$. Figure 6(c) shows the spatial structure of the horizontal density gradient field filtered at the superharmonic frequency $2\omega_{\text{res}}$ for the same experiment. The observed wave field at the superharmonic frequency $2\omega_{\text{res}}$, shows a clean mode-1 spatial structure which is propagating only in the upper section of the vertical fluid column as $1 < 2\omega_{\text{res}}/N_{\min} < \beta$. This experimental observation validates the theoretical prediction of triadic resonant interaction of mode-3 and mode-4 at $\omega_{\text{res}}/N_{\min} = 0.8571$ for $\beta = 2.1$, exciting a superharmonic mode-1.

Experiments were also performed at several other off-resonant frequencies to identify the frequency range (around the resonant frequency) over which a superharmonic mode-1 is excited, and also to identify the resonant peak frequency. The normalized strength of the superharmonic signal $\widehat{A_{2\omega_0}/A_{\omega_0}}$ (strength here refers to the amplitude of the horizontal density gradient, filtered at the respective frequency), is computed for all the forcing frequencies for each stratification profile considered (i.e., for every value of β considered), where $A_{2\omega_0}$ and A_{ω_0} are the strengths/amplitudes of the signal filtered at the superharmonic frequency $2\omega_0$ and the forcing frequency ω_0, respectively. It is important to compute a normalized quantity ($A_{2\omega_0}/A_{\omega_0}$) as a fixed horizontal displacement of the plates (5 mm or 10 mm) of the wave generator at different forcing frequencies does not correspond to a same amplitude of forcing for the horizontal density gradient field (the quantity measured using synthetic Schlieren technique). The normalized strength of the superharmonic signal is re-normalized to compare across various β or the stratification profiles setup in the experiments. The re-normalization is defined as $\widehat{X} = X/\max(X)$. The solid red curve in Fig. 7(a) shows the variation of the renormalized strength of the superharmonic signal ($\widehat{A_{2\omega_0}/A_{\omega_0}}$) for $\beta = 2.1$ with the
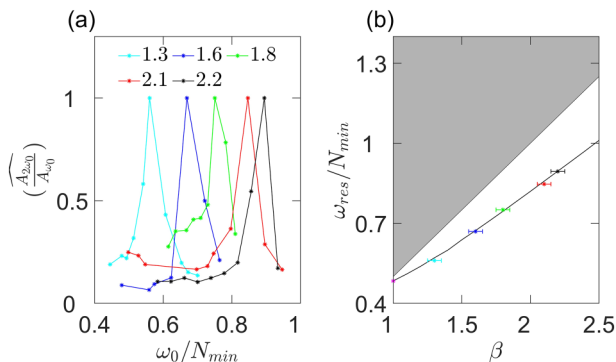
FIG. 7. (a) Variation of renormalized strength of the superharmonic wave ($\widehat{A_{2\omega_0}/A_{\omega_0}}$) with forcing frequency $\omega_0/N_{\min}$ for five different values of β (tabulated in Table I). (b) The resonant peak frequencies from plot (a) plotted over the theoretically expected resonant frequency curve $\omega_{res}/N_{\min}$ as in Fig. 5(b).

forcing frequency (around the expected resonant frequency). A clear resonant peak is identified very close to the theoretical predicted value $\omega_{res}/N_{\min} = 0.8571$.

Experiments were also performed for various stratification profiles with values of β in the range $1 < \beta < 2.5$ for a range of forcing frequencies around the theoretically predicted resonant forcing frequency. Figure 7(a) shows the resonant/off-resonant strength of the renormalized superharmonic signal ($\widehat{A_{2\omega_0}/A_{\omega_0}}$), for the five stratification profiles with different values of β (see Table I). The resonant peaks are observed for all the five values of β, with peak frequency $\omega_{res}/N_{\min}$ shifting toward the right (as seen in Fig. 7(a) with an increase in the value of β. In Fig. 7(b), the solid black line corresponds to the theoretical prediction of the variation of resonant peak frequency with β, same as shown by black curve in Fig. 5(b). The observed resonant peak frequencies are plotted as points in colors corresponding to the color of the resonant peak in Fig. 7(a). Error bars are plotted for each value of β, associated with computing the linear fit $N(z)$ profile as discussed in Sec. III. The experimentally observed resonant peak frequencies have close agreement with the theoretically predicted values of resonant peak frequencies $\omega_{res}/N_{\min}$ within the limits of the experimental errors. All the experiments performed for resonant cross-modal interactions of mode-3 and mode-4 resulting in excitation of mode-1 superharmonic internal wave, clearly capture the resonant peak frequencies predicted by the weakly nonlinear theory for all values of β considered.

2. Superharmonic mode-2

In a finite-depth nonuniform stratification, its not necessary for the superharmonic mode excited by resonant interaction of (m, n) at frequency ω_0 to be mode-$|m - n|$ [23]. For a prescribed stratification corresponding to a given value of β, depending on the range of forcing frequencies, modes other than mode-$|m - n|$ could also be excited due to superharmonic resonant interaction. To explore this possibility, experiments were also performed at and around the resonant frequency $\omega_{res}/N_{\min}$, at which mode-3 and mode-4 at $\omega_{res}/N_{\min}$ would resonantly interact to excite a superharmonic mode-2 at $2\omega_{res}/N_{\min}$.

For a prescribed stratification with $\beta = 2.1$, the superharmonic wave amplitude $|h_{34}^{\max}|$ diverges at $\omega_{res}/N_{\min} = 0.6743$ corresponding to a mode-2 superharmonic internal wave. For the same stratification profile as shown in Fig. 4 corresponding to $\beta = 2.1$, experiments were performed by forcing mode-3 and mode-4 at $\omega_{res}/N_{\min} = 0.6743$ at the left end of the tank. Figure 8(a) shows the instantaneous horizontal density gradient field at $t = 20T_0$ as forced by the wave generator from $x = 0$. The horizontal density gradient field filtered at the resonant forcing frequency $\omega_{res}/N_{\min} = 0.6743$ shows primary wave field to be composed of the forcing modes, mode-3 and mode-4 [shown in Fig. 8(b)]. When the horizontal density gradient field is filtered at $\omega_{res}/N_{\min}$ as shown in Fig. 8(c),
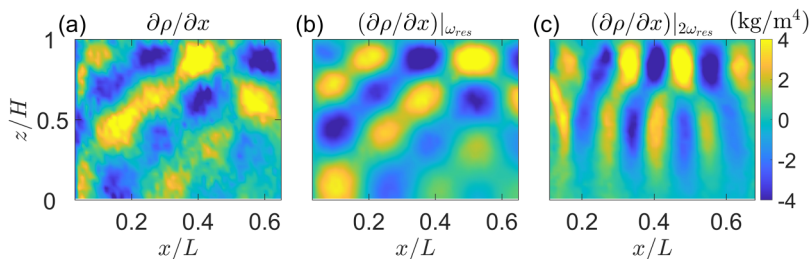
FIG. 8. Horizontal density gradient wave-fields for the cross-modal interaction, i.e., $(m, n, p) = (3, 4, 2)$, at the resonant forcing frequency of $\omega_{\text{res}}/N_{\min} = 0.6743$. (a) Instantaneous horizontal density gradient field, (b) Horizontal density gradient field filtered at the forcing frequency $\omega_{\text{res}}/N_{\min}$, and (c) Horizontal density gradient field filtered at the superharmonic frequency $2\omega_{\text{res}}/N_{\min}$. All plots are to $t = 20T_0$, where $T_0 = 2\pi/\omega_{\text{res}}$.

the wave field shows a mode-2 structure as we move away from the wave generator at $x = 0$. So indeed the resonant interaction of mode-3 and mode-4 at $\omega_{\text{res}}/N_{\min}$ excites a superharmonic mode-2 at $2\omega_{\text{res}}/N_{\min}$, which was not a possibility in a uniform stratification. Depending on the forcing resonant frequency $\omega_{\text{res}}/N_{\min}$, mode-3 and mode-4 can resonantly interact to excite a mode-1 or mode-2 superharmonic internal wave.

B. Self-interaction

In a nonuniform stratification, self-interaction of a mode at a prescribed $\omega_0/N_{\min}$ could also result in resonant excitation of a superharmonic mode which is inhibited for the case of a uniform stratification $[N(z) = N_{\min}]$ [16]. This suggests that individual modes can inherently become unstable by resonant self-interactions resulting in excitation of superharmonic modes at frequency $2\omega/N_{\min}$. To investigate the resonant self-interaction of isolated modes in our experiments, two cases are considered (i) resonant self-interaction of a mode-3 exciting mode-1 superharmonic and (ii) resonant self-interaction of a mode-4 exciting mode-1 superharmonic. In Secs. IV B 1 and IV B 2, the experimental results from the resonant self-interaction of an isolated mode-3 and mode-4 are discussed, respectively.

1. Mode-3 self-interaction

For the same stratification profile $\beta = 2.1$ as discussed in the previous Sec. IV A and as shown in Fig. 4, the superharmonic wave amplitude $|h_{33}^{\max}|$ due to self-interaction of mode-3 diverges at $\omega_{\text{res}}/N_{\min} = 0.8326$. Experiments are performed with isolated mode-3 being forced at $\omega_{\text{res}}/N_{\min} = 0.8326$, with the wave generator at the left end of the tank. Figure 9(a) shows a snapshot of the instantaneous horizontal density gradient wave field for an isolated mode-3 forced at the expected resonant frequency of $\omega_{\text{res}}/N_{\min} = 0.8326$. The horizontal density gradient field filtered at the forcing frequency ω_{res} as shown in Fig. 9(b), displays a spatial structure corresponding to a clear isolated mode-3 as forced at $x = 0$. Figure 9(c) shows the spatial structure of the horizontal density gradient field filtered at the superharmonic frequency $2\omega_{\text{res}}$ for the same experiment. The observed wave field at the superharmonic frequency $2\omega_{\text{res}}$, shows a clean mode-1 spatial structure which is propagating only in the upper section of the vertical fluid column (as $1 < 2\omega_{\text{res}}/N_{\min} < \beta$) as we move further away from $x = 0$. This result experimentally validates the theoretical prediction of triadic resonant interaction of an isolated mode-3 at $\omega_{\text{res}}/N_{\min} = 0.8326$ for $\beta = 2.1$, exciting a superharmonic mode-1.

2. Mode-4 self-interaction

As discussed in previous Sec. IV B 1 where a mode-3 resonantly self-interacted to excite a mode-1 superharmonic internal wave, even a mode-4 could resonantly interact to excite a mode-1
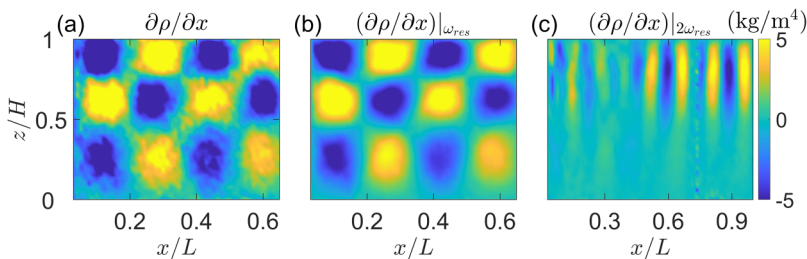
FIG. 9. Horizontal density gradient wave-fields for the self interaction, i.e., $(m, n, p) = (3, 3, 1)$, at the resonant forcing frequency of $\omega_{res}/N_{min} = 0.8326$. (a) Instantaneous horizontal density gradient field, (b) Horizontal density gradient field filtered at the forcing frequency ω_{res}/N_{min}, and (c) Horizontal density gradient field filtered at the superharmonic frequency $2\omega_{res}/N_{min}$. All the plots correspond to $t = 20T_0$, where $T_0 = 2\pi/\omega_{res}$.

superharmonic internal wave. For $\beta = 3$, the superharmonic wave amplitude $|h_{44}^{max}|$ diverges at $\omega_{res}/N_{min} = 1.2368$. An isolated mode-4 was forced using the wave generator at forcing frequency $\omega_{res}/N_{min} = 1.2368$. Figure 10(a) shows a snapshot of the instantaneous horizontal density gradient wave field for an isolated mode-4 forced at $x = 0$. The horizontal density gradient field filtered at the forcing frequency ω_{res} is shown in Fig. 10(b), displays a spatial structure corresponding to a clear isolated mode-4 as forced at the left end of the tank at $x = 0$. Figure 10(c) shows the spatial structure of the horizontal density gradient field filtered at the superharmonic frequency $2\omega_{res}$ for the same experiment. The observed wave field at the superharmonic frequency $2\omega_{res}$, shows a clean mode-1 spatial structure which is propagating only in the upper section of the vertical fluid column as $1 < 2\omega_{res}/N_{min} < \beta$. This result experimentally validates the theoretical prediction of triadic resonant interaction of an isolated mode-4 at $\omega_{res}/N_{min} = 1.2368$ for $\beta = 3$, exciting a superharmonic mode-1. This provides an experimental evidence for self-interaction of an isolated modes exciting superharmonic internal waves in finite-depth nonuniform stratifications.

V. RESULTS: OCEANLIKE NONUNIFORM STRATIFICATION PROFILE

In this section, an idealized oceanlike nonuniform stratification profile with a pycnocline is considered. As done in the preceding sections, the cross-modal interaction of mode-3 with mode-4, and the self-interaction of mode-3 are considered. We present results for an oceanlike nonuniform stratification profile $N_1(z)$ defined [as in Eq. (10)] by

$$\frac{N_1(z)}{N_{min}} = 1 + (\beta - 1)\exp\left(-\frac{(z - z_c)^2}{\sigma^2}\right), \tag{12}$$

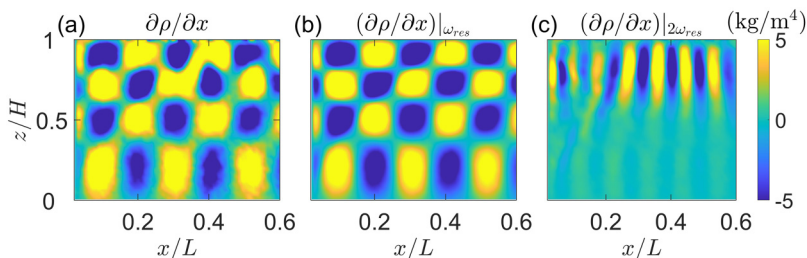
FIG. 10. Horizontal density gradient wave-fields for the self interaction, i.e., $(m, n, p) = (4, 4, 1)$, at the resonant forcing frequency of $\omega_{res}/N_{min} = 1.2368$. (a) Instantaneous horizontal density gradient field, (b) Horizontal density gradient field filtered at the forcing frequency ω_{res}/N_{min}, and (c) Horizontal density gradient field filtered at the superharmonic frequency $2\omega_{res}/N_{min}$. All the plots correspond to $t = 20T_0$, where $T_0 = 2\pi/\omega_{res}$.
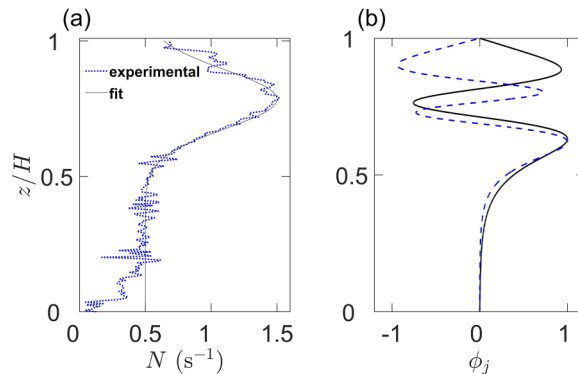
FIG. 11. (a) A measured stratification profile (blue dotted line) along with the fitted $N(z)$ profile (black solid line) corresponding to $N_1(z)$ fit with $\beta = 3$ [as in Eq. (12)]. (b) Mode-3 (black solid curve) and mode-4 (blue dashed curve) for $\beta = 3$ at $\omega_0/N_{min} = 1.3705$.

where N_{min} is the deep ocean uniform stratification and z_c is the center of the pycnocline whose characteristic width is σ. This idealized oceanlike nonuniform stratification profile has been considered in various previous studies relevant to ocean [17,23,25,30,44]. The mode shapes for such a nonuniform stratification [as in Eq. (12)] assume a sinusoidal form in the uniformly stratified deep ocean, and contain smaller vertical length scales in the pycnocline region. For the results discussed in this section, experiments were setup with a stratification profile corresponding to $\beta = 3$, with a pycnocline centered at $z_c/H = 0.8$ with a pycnocline width of $\sigma/H = 0.15$. Dotted line in Fig. 11(a) shows the measured stratification profile setup in the tank and the solid line is the fit $N_1(z)$ profile for $\beta = 3$ and $N_{min} = 0.5$. The mode shapes of the primary wave modes, mode-3 and mode-4 corresponding to forcing frequency of $\omega_0/N_{min} = 1.3705$ are shown in Fig. 4(b). The experimental results for cross-modal interaction of mode-3 and mode-4, and self-interaction of mode-3 are presented in the preceding subsections.

A. Cross-modal interaction

For the nonuniform stratification profile considered, mode-3 and mode-4 resonantly self-interact to excite a mode-1 superharmonic internal wave at resonant peak frequency $\omega_{res}/N_{min} = 1.3705$ (obtained from the divergence of superharmonic wave amplitude $|h_{34}^{max}|$). Mode-3 and mode-4 at $\omega_{res}/N_{min} = 1.3705$ are forced at the left end of the tank using the wave generator. Figure 12(a)
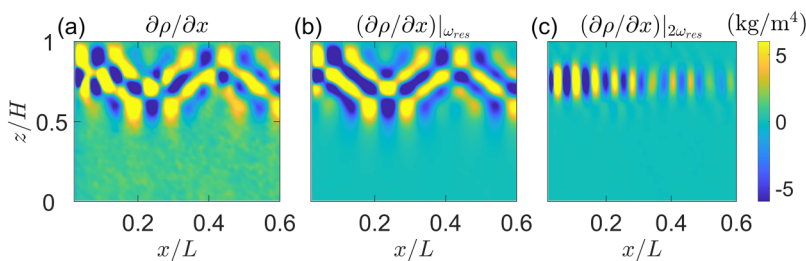

FIG. 12. Horizontal density gradient fields for the cross-modal interaction, i.e., $(m, n, p) = (3, 4, 1)$ at the resonant frequency $\omega_{res}/N_{min} = 1.3705$ for a nonuniform stratification with a pycnocline. (a) Instantaneous horizontal density gradient field, (b) Horizontal density gradient field filtered at the forcing frequency ω_{res}/N_{min}, and (c) Horizontal density gradient field filtered at the superharmonic frequency $2\omega_{res}/N_{min}$. All the plots correspond to $t = 20T_0$, where $T_0 = 2\pi/\omega_{res}$.
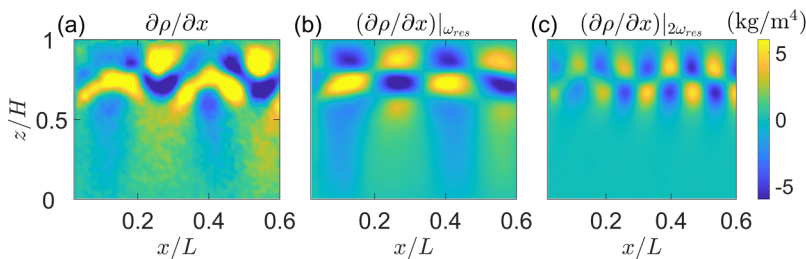
FIG. 13. Horizontal density gradient fields for the self-interaction, i.e., $(m, n, p) = (3, 3, 2)$ at the resonant frequency $\omega_{\text{res}}/N_{\min} = 0.6842$ for a nonuniform stratification with a pycnocline. (a) Instantaneous horizontal density gradient field, (b) Horizontal density gradient field filtered at the forcing frequency $\omega_{\text{res}}/N_{\min}$, and (c) Horizontal density gradient field filtered at the superharmonic frequency $2\omega_{\text{res}}/N_{\min}$. All the plots correspond to $t = 20T_0$, where $T_0 = 2\pi/\omega_{\text{res}}$.

shows a snapshot of the instantaneous horizontal density gradient wave field at $t = 20T_0$, where $T_0 = 2\pi/\omega_{\text{res}}$. The horizontal density gradient field filtered at the forcing frequency $\omega_{\text{res}}/N_{\min} = 1.3705$ as shown in Fig. 12(b), displays a spatial structure of wave field corresponding to a superposition of mode-3 and mode-4 propagating only in the pycnocline region. Figure 12(c) shows the spatial structure of the horizontal density gradient field filtered at the superharmonic frequency $2\omega_{\text{res}}$ for the same experiment. The observed wave field at the superharmonic frequency $2\omega_{\text{res}}$, shows a very clean mode-1 spatial structure which is trapped in the pycnocline region. This experimental observation indeed validates the theoretical prediction of triadic resonant interaction of mode-3 and mode-4 at $\omega_{\text{res}}/N_{\min} = 1.3705$ exciting a superharmonic mode-1, for the oceanlike nonuniform stratification profile considered.

B. Self-interaction

Using the same nonuniform stratification profile as in the previous Sec. V A, experiments were performed for resonant self-interaction of a mode-3 exciting a mode-2 superharmonic internal wave, at the corresponding resonant peak frequency $\omega_{\text{res}}/N_{\min} = 0.6842$. An isolated mode-3 is forced with the prescribed mode shape corresponding the nonuniform stratification profile using the wave generator. Figure 13(a) shows a snapshot of the instantaneous horizontal density gradient wave field for an isolated mode-3 forced at $x = 0$. The horizontal density gradient field filtered at the forcing frequency ω_{res} is shown in Fig. 13(b), displays a spatial structure corresponding to a clear isolated mode-3 as forced at the left end of the tank at $x = 0$. Figure 13(c) shows the spatial structure of the horizontal density gradient field filtered at the superharmonic frequency $2\omega_{\text{res}}$ for the same experiment. The observed wave field at the superharmonic frequency $2\omega_{\text{res}}$, shows a very clean mode-2 spatial structure which is trapped in the pycnocline region. This result experimentally validates the theoretical prediction of triadic resonant interaction of isolated mode-3 at $\omega_{\text{res}}/N_{\min} = 0.6842$ exciting a mode-2 superharmonic internal wave for the oceanlike nonuniform stratification profile considered.

VI. CONCLUSIONS

Experiments were performed to investigate the excitation of superharmonic internal wave modes by nonlinear interactions of internal waves in finite-depth nonuniform stratifications. Two cases were considered: (i) cross-modal interaction resulting from interaction of two different modes at same frequency and (ii) self-interaction of an isolated mode. In both cases, the excitation of superharmonic internal wave mode at twice the resonant forcing frequency due to resonant interactions of internal wave modes was observed in the experiments. Cross-modal interaction of internal wave modes (m, n) at frequency ω_0 resulting in excitation of superharmonic mode other than the

mode-$|m - n|$ was also observed in the experiments, which is inhibited for a uniform stratification. Resonant self-interaction of an isolated mode exciting a superharmonic internal wave mode was observed, which is a possibility for a nonuniform stratification only. The resonant peak frequency ω_{res}/N_{min} was well captured by performing experiments over a range of forcing frequencies, and was in close agreement with the theoretically predicted resonant peak frequency obtained using the weakly nonlinear framework. The theoretical prediction for the variation of the resonant peak frequency with β (a characteristic measure of the strength of nonuniformity in stratification) was well captured in the experiments performed for various values of β [Fig. 7(b)].

Finally, experiments were also performed for an idealized oceanlike stratification profile with a pycnocline, to study both cross-modal interactions and self-interactions. For a nonuniform stratification profile with a pycnocline, the resonantly excited superharmonic internal wave modes were found to be trapped in the pycnocline region. The trapping of superharmonics in the pycnocline region was also observed in the earlier experimental study of Wunsch *et al.* [29], when an internal wave beam (from the bottom) impinges on the pycnocline. The excitation of low mode higher harmonics in experiments [29] could either be by cross-modal interaction or by self-interaction of internal waves depending on how close the forcing frequency is to the resonant frequency of the nonlinear interactions between the constituent internal wave modes in the incident wave beam (as discussed in Sec. 4.2 of Varma and Mathur [23]). Recent theoretical study by Wunsch and Marcellino [26] shows the relevance of excitation of higher harmonics by triadic resonant interactions in different parts of the ocean by considering global ocean stratification profiles measured by ARGO floats.

Further studies considering internal wave modes at smaller forcing frequencies in the primary wave field, with a nonuniform stratification profile with pycnocline could be more relevant to various internal waves phenomena in the ocean like topographic scattering/generation of internal tides, propagation of low modes away from the generation sites and generation of near inertial waves in the presence of background rotation. The current study also raises important questions on the validity of linear models that assume the presence of multiple modes at a given frequency, which is often the case in the ocean. Including the effects of background rotation, effects of finite-shear and considering a stratification profile from in-situ observations in the ocean, in the future studies could give more insights.

[1] A. E. Gill, *Atmosphere-Ocean Dynamics* (Academic Press, San Diego, CA, 1982), Vol. 30.

[2] R. D. Ray and G. T. Mitchum, Surface manifestation of internal tides in the deep ocean: Observations from altimetry and island gauges, Prog. Oceanogr. **40**, 135 (1997).

[3] Z. Zhao, M. H. Alford, and J. B. Girton, Mapping low-mode internal tides from multisatellite altimetry, Oceanography **25**, 42 (2012).

[4] C. Garrett and E. Kunze, Internal tide generation in the deep ocean, Annu. Rev. Fluid Mech. **39**, 57 (2007).

[5] T. S. Johnston and M. A. Merrifield, Internal tide scattering at seamounts, ridges, and islands, J. Geophys. Res.: Oceans **108** (2003).

[6] E. Kunze and S. L. Smith, The role of small-scale topography in turbulent mixing of the global ocean, Oceanography **17**, 55 (2004).

[7] L. St. Laurent and C. Garrett, The role of internal tides in mixing the deep ocean, J. Phys. Oceanogr. **32**, 2882 (2002).

[8] C. Staquet and J. Sommeria, Internal gravity waves: From instabilities to turbulence, Annu. Rev. Fluid Mech. **34**, 559 (2002).

[9] A. Tabaei, T. Akylas, and K. G. Lamb, Nonlinear effects in reflecting and colliding internal wave beams, J. Fluid Mech. **526**, 217 (2005).

[10] S. Sarkar and A. Scotti, From topographic internal gravity waves to turbulence, Annu. Rev. Fluid Mech. **49**, 195 (2017).

[11] K. Hasselmann, A criterion for nonlinear wave stability, J. Fluid Mech. **30**, 737 (1967).

[12] R. E. Davis and A. Acrivos, The stability of oscillatory internal waves, J. Fluid Mech. **30**, 723 (1967).

[13] T. Dauxois, S. Joubaud, P. Odier, and A. Venaille, Instabilities of internal gravity wave beams, Annu. Rev. Fluid Mech. **50**, 131 (2018).

[14] B. Fan and T. Akylas, Instabilities of finite-width internal wave beams: From floquet analysis to psi, J. Fluid Mech. **913**, A5 (2021).

[15] D. Varma, M. Mathur, and T. Dauxois, Instabilities in internal gravity waves, Math. Eng. **5**, 1 (2023).

[16] S. A. Thorpe, On wave interactions in a stratified fluid, J. Fluid Mech. **24**, 737 (1966).

[17] D. Varma, V. K. Chalamalla, and M. Mathur, Spontaneous superharmonic internal wave excitation by modal interactions in uniform and nonuniform stratifications, Dynam. Atmos. Ocean **91**, 101159 (2020).

[18] P. Husseini, D. Varma, T. Dauxois, S. Joubaud, P. Odier, and M. Mathur, Experimental study on superharmonic wave generation by resonant interaction between internal wave modes, Phys. Rev. Fluids **5**, 074804 (2020).

[19] S. Boury, T. Peacock, and P. Odier, Experimental generation of axisymmetric internal wave superharmonics, Phys. Rev. Fluids **6**, 064801 (2021).

[20] S. Thorpe, Nonlinear reflection of internal waves at a density discontinuityat the base of the mixed layer, J. Phys. Oceanogr. **28**, 1853 (1998).

[21] J. McHugh, Internal waves at an interface between two layers of differing stability, J. Atmos. Sci. **66**, 1845 (2009).

[22] S. Wunsch, Nonlinear harmonic generation by diurnal tides, Dynam. Atmos. Ocean **71**, 91 (2015).

[23] D. Varma and M. Mathur, Internal wave resonant triads in finite-depth non-uniform stratifications, J. Fluid Mech. **824**, 286 (2017).

[24] S. Wunsch, Harmonic generation by nonlinear self-interaction of a single internal wave mode, J. Fluid Mech. **828**, 630 (2017).

[25] S. Gururaj and A. Guha, Resonant and near-resonant internal wave triads for non-uniform stratifications. Part 2. Vertically bounded domain with mild-slope bathymetry, J. Fluid Mech. **943**, A33 (2022).

[26] S. Wunsch and F. J. Marcellino, Estimates of mode-1 internal tide harmonic generation in the global ocean, Phys. Rev. Fluids **8**, 124801 (2023).

[27] M. J. Mercier, M. Mathur, L. Gostiaux, T. Gerkema, J. M. Magalhães, J. C. Da Silva, and T. Dauxois, Soliton generation by internal tidal beams impinging on a pycnocline: Laboratory experiments, J. Fluid Mech. **704**, 37 (2012).

[28] S. Wunsch and A. Brandt, Laboratory experiments on internal wave interactions with a pycnocline, Exp. Fluids **53**, 1663 (2012).

[29] S. Wunsch, I. Delwiche, G. Frederick, and A. Brandt, Experimental study of nonlinear harmonic generation by internal waves incident on a pycnocline, Exp. Fluids **56**, 87 (2015).

[30] N. Grisouard, C. Staquet, and T. Gerkema, Generation of internal solitary waves in a pycnocline by an internal wave beam: A numerical study, J. Fluid Mech. **676**, 491 (2011).

[31] P. Diamessis, S. Wunsch, I. Delwiche, and M. Richter, Nonlinear generation of harmonics through the interaction of an internal wave beam with a model oceanic pycnocline, Dynam. Atmos. Ocean **66**, 110 (2014).

[32] B. R. Sutherland, Excitation of superharmonics by internal modes in non-uniformly stratified fluid, J. Fluid Mech. **793**, 335 (2016).

[33] L. E. Baker and B. R. Sutherland, The evolution of superharmonics excited by internal tides in nonuniform stratification, J. Fluid Mech. **891**, R1 (2020).

[34] B. R. Sutherland and M. S. Dhaliwal, The nonlinear evolution of internal tides. Part 1: The superharmonic cascade, J. Fluid Mech. **948**, A21 (2022).

[35] P. H. LeBlond and L. A. Mysak, *Waves in the Ocean* (Elsevier, Amsterdam, 1981).

[36] G. Oster, Density gradients, Sci. Am. **213**, 70 (1965).

[37] D. Hill, General density gradients in general domains: The "two-tank" method revisited, Exp. Fluids **32**, 434 (2002).

[38] M. Economidou and G. Hunt, Density stratified environments: The double-tank method, Exp. Fluids **46**, 453 (2009).

[39] M. J. Mercier, D. Martinand, M. Mathur, L. Gostiaux, T. Peacock, and T. Dauxois, New wave generation, J. Fluid Mech. **657**, 308 (2010).

[40] Y. Dossmann, F. Pollet, P. Odier, and T. Dauxois, Mixing and formation of layers by internal wave forcing, J. Geophys. Res.: Oceans **122**, 9906 (2017).

[41] S. Dalziel, G. O. Hughes, and B. R. Sutherland, Whole-field density measurements by 'synthetic schlieren', Exp. Fluids **28**, 322 (2000).

[42] A. Fincham and G. Delerce, Advanced optimization of correlation imaging velocimetry algorithms, Exp. Fluids **29**, S013 (2000).

[43] J. Sommeria, Uvmat toolbox for matlab, Tech. Rep. (LEGI/CNRS-UJF-INPG, http://coriolis.legi.grenoble-inp.fr).

[44] M. Mathur, G. S. Carter, and T. Peacock, Topographic scattering of the low-mode internal tide in the deep ocean, J. Geophys. Res.: Oceans **119**, 2165 (2014).